Polymer 84 (2016) 138–147

Contents lists available at ScienceDirect

Polymer

journal homepage: www.elsevier.com/locate/polymer

Morphology and opto-thermal properties of the thermo-responsive PNIPAAm-protected gold nanorods

Chia-Fen Lee [a], Geng-Ming Zhang [b], Mu-Ping Nieh [c], Trong-Ming Don [b, *]

[a] Department of Cosmetic Science, Institute of Cosmetic Science, Chia Nan University of Pharmacy and Science, Tainan, 71710, Taiwan
[b] Department of Chemical and Materials Engineering, Tamkang University, Tamsui District, New Taipei City, 25137, Taiwan
[c] Polymer Program, Institute of Materials Science, University of Connecticut, Storrs, CT, 06269, USA

ARTICLE INFO

Article history:
Received 2 November 2015
Received in revised form
20 December 2015
Accepted 25 December 2015
Available online 29 December 2015

Keywords:
poly(*N*-isopropyl acrylamide)
Gold nanorods
Thermo-responsive
Opto-thermal effect

ABSTRACT

In this study, thermo-responsive poly(*N*-isopropyl acrylamide)-*g*-gold nanorods (PNIPAAm-*g*-GNRs) were prepared by grafting telechelic PNIPAAm-SH to the GNRs. They were stable in aqueous medium where the GNRs were protected by PNIPAAm chains as revealed by transmission electron microscope. The longitudinal surface plasmon absorbance had a red shift to 810 nm, and the lower critical solution temperature (LCST) of the PNIPAAm was increased to 34.9 °C. After being irradiated by near-IR for 5 min, the PNIPAAm-*g*-GNRs solution indicated a temperature increment above its LCST. The opto-thermal effect thus could induce the morphology change of the PNIPAAm, which was found to be reversible. Furthermore, the PNIPAAm-*g*-GNRs had a much lower cytotoxicity than the surfactant-stabilized GNRs. The cell viability of fibroblast after two days of culture could still reach 89.0% relative to the control. Therefore, the PNIPAAm-*g*-GNRs could be used as drug carriers in which the drug-release could be controlled by remote near-IR.

1. Introduction

In recent years, gold nanoparticles (AuNPs) have attracted much attention because of their unique properties derived from the quantum-scale dimension. AuNPs can be applied in the fields of drug delivery, photodynamic therapy, and diagnostic imaging [1–6]. Not only AuNPs with different sizes can be synthesized, but also with different shapes such as spheres, rods, platelets, polyhedrons, and multipods [7–15]. Among them, gold nanorods (GNRs) have attracted special interest owing to their unique optical properties. With a suitable aspect ratio and the resulting longitudinal surface plasmon resonance (SPR), GNRs can exhibit an absorption band in the near-infrared (NIR) region [15], and thus induce opto-thermal conversion. This is beneficial for biomedical applications especially in the hyperthermic therapy in consideration of the penetration of NIR light into biological tissues [2–6]. However, pure AuNPs including GNRs are not stable in aqueous medium due to self-aggregation. They are generally stabilized by surfactants such as cetyltrimethylammonium bromide (CTAB). These surfactants can be replaced by alkanethiols [16–18] and thiolated polymers [19–25] that can be chemically bonded to the AuNPs, where the thiolated polymers have been proved to be more efficient for stabilizing the AuNPs [24,25]. The thiolated polymers can have different architectures and even different functional properties to extend the applications of polymer-protected AuNPs in various fields. One of the functional polymers that has been studied and applied in various fields is poly(*N*-isopropylacrylamide) (PNIPAAm), a thermo-responsive polymer which can exhibit a phase transition at the lower critical solution temperature (LCST). In other words, PNIPAAm is hydrophilic and dissolves in water at temperatures below the LCST, but becomes hydrophobic and precipitates out from the solution when above this temperature [26,27]. In addition, various hydrophilic or hydrophobic co-monomers can be added during polymerization to produce PNIPAAm copolymers with tunable LCST [28,29]. PNIPAAm and its copolymers thus have potential as controlled drug-release carriers in which the encapsulated drug can be expelled from the carriers as they undergo volume-shrinkage once the environmental temperature is raised to above their respective LCSTs. Many researchers have tried to endow the AuNPs with thermo-responsive properties in order to extend their applications. Thermo-responsive colloid particles or nanocomposites based on PNIPAAm and AuNPs mostly in spherical shape have thus been

* Corresponding author.
E-mail address: tmdon@mail.tku.edu.tw (T.-M. Don).

http://dx.doi.org/10.1016/j.polymer.2015.12.047
0032-3861/

investigated [30–35]. Contreras-Cáceres et al. [30] prepared thermo-responsive nanocomposites comprising a gold nanoparticle core and a PNIPAAm shell. They varied the crosslinking density of the PNIPAAm shell as well as the shell thickness from a few to several hundred nanometers. Chen et al. [31] demonstrated that patterned, thermo-responsive PNIPAAm brushes could be used as motor arrays to manipulate the movement of AuNPs in response to external stimuli that induced a conformational change in the brushes as the driving force. Li et al. [32] prepared thermo-responsive nanocomposites based on gold nanocages covered with PNIPAAm which could be used for high-intensity focused ultrasound-induced drug release. Zhao et al. [33] synthesized the hybrid material with a core–shell structure in which the PNIPAAm hydrogel was chemically grafted onto the spherical AuNPs. Kim et al. [34] used the method of free radical polymerization to polymerize NIPAAm and acrylic acid (AA) in the presence of the gold-shell/silica-core particles to obtain the composite nanoparticles, in which the thermo-responsive poly(NIPAAm-co-AA) hydrogel would be coated on the surface of gold-shell/silica-core particles. Raula et al. [35] also reported the synthesis of AuNPs grafted with the PNIPAAm by surface-induced reversible addition–-fragmentation chain transfer (RAFT) polymerization.

Moreover, hybrid colloids consisting of GNRs with the thermo-responsive PNIPAAm as well as its derivatives have also been prepared [36–40]. The beneficial is that the temperature-rise being able to induce the morphology change of the PNIPAAm can be achieved by irradiation of NIR on the hybrid material. Consequently, this is due to the SPR effect from the conjugated GNRs. Karg et al. [36] synthesized the thermo-responsive composite colloids consisting of poly(NIPAAm-co-allylacetic acid) microgel cores and GNRs assembled on their surface. They found that the composite colloids were not only thermosensitive but also pH-sensitive, owing to the copolymerization of allylacetic acid with NIPAAm. Almost with the same core-and-attached GNR structure, Khan and Alhoshan [37] used N,N′-methylene bisacrylamide as a crosslinker during the synthesis of the NIPAAm and AA to produce negative-charged microgel particles by the method of surfactant-free emulsion polymerization. Subsequently, the CTAB-stabilized GNRs were added and mixed with the swollen microgel particles to prepare hybrid material. The transmission electron micrographs confirmed that the GNRs were attached to the surface of the microgel particles by the electrostatic interactions between the oppositely charged particles. On the other hand, Shang et al. [38] synthesized the nanogels composed of GNR and PNIPAAm copolymer in two steps. A poly(ethylene glycol)-methacrylate (PEGMA) monolayer was first attached on the surface of GNR, followed by in-situ polymerization and crosslinking of this PEGMA with NIPAAm monomer. They reported that the LCST of the prepared nanogel of GNR/poly(NIPAAm-co-PEGMA) could be tuned by changing the molar ratio of NIPAAm/PEGMA. Besides, the NIR-mediated drug-release behavior and photodynamic therapy effect on Hela cells of the produced nanogel were studied. Though composite colloids consisting of PNIPAAm and GNR have been studied, there are not many reports about PNIPAAm-protected GNRs by directly chemical-grafting PNIPAAm chains to GNRs [41,42]. Wei et al. [41] synthesized the thermo-responsive nanohybrids by grafting the PNIPAAm from the GNRs using the method of surface-initiated atom transfer radical polymerization (SI-ATRP). They showed that the nanohybrids had a distinct core–shell structure. Nguyen et al. [42] investigated the hybrid plasmonic core–shell system made of lithographic GNRs and coated by a PNIPAAm shell. The PNIPAAm was also grafting from the initiator-covered GNRs using the same method of SI-ATRP. They concluded that the use of PNIPAAm-protected GNRs could be applied spanning from opto-mechanical modulators to nanoscale adhesion and molecular sensing. Instead of using "grafting-from" method, the "grafting-to" method was adopted in this study to prepare the PNIPAAm-protected GNRs. First, PNIPAAm-SH was synthesized via free radical polymerization of PNIPAAm-COOH followed by coupling with the thiol-bearing molecule. This method was similar to that reported by Shan et al. [25] The PNIPAAm-SH was then chemically bonded to the GNRs at different amounts to produce PNIPAAm-protected GNRs, designated as PNIPAAm-*g*-GNRs. Their structure, morphology, phase behavior and opto-thermal properties were then investigated.

2. Experimental

2.1. Materials

N-isopropyl acrylamide (NIPAAm) as monomer, cysteamine hydrochloride (or 2-mercaptoethylamine hydrochloride, $HSCH_2CH_2NH_2$), *N*-hydroxysuccinimide (NHS), hydrogen tetrachloroaurate (III) trihydrate ($HAuCl_4 \cdot 3H_2O$), cetyltrimethylammonium bromide (CTAB) and ascorbic acid (AA) were all purchased from Acros Organics (Geel, Belgium). *N*-(3-dimethylaminopropyl)-*N*′-ethylcarbodiimide hydrochloride (EDC), 4,4′-azobis(4-cyanopentanoic acid) (ACPA) as initiator, sodium borohydride ($NaBH_4$), and 5,5′-dithiobis(2-nitrobenzoic acid) (DTNB) were supplied by Aldrich (Missouri, USA). All other chemicals were at least analytical grade and used without further purification.

2.2. Synthesis of PNIPAAm-COOH

The preparation of PNIPAAm-COOH and PNIPAAm-SH followed the method of Shan et al. [25] with a slight modification. NIPAAm monomer (30 mmol) was dissolved in ethanol (25 mL, 99.5%) with stirring; the solution was then heated to 70 °C and purged with nitrogen. The azo initiator (ACPA, 0.5 mmol), dissolved in another 5 mL ethanol, was added to the monomer solution. The ACPA was thermally decomposed to two 4-cyanopentanoic acid radicals (•CPA) with the elimination of nitrogen. The •CPA then attacked the monomer to initiate free-radical polymerization. The reaction is shown in route (1), Scheme 1. Because of the bulky side group and also for brevity, only one CPA group attached to the PNIPAAm chain is shown in route (1). It is possible that some macromolecular chains had two CPA end groups. The bonded CPA thus provided terminal carboxylic acid group on the polymer chains.

After 12 h of reaction, the reaction solution was quenched in ice-water and the ethanol was removed by a rotary evaporator at room temperature to obtain the reaction product, PNIPAAm-COOH. For purification, it was re-dissolved in acetone and precipitated by the addition of excess ether, followed by centrifugation. The purification process was repeated twice. Finally, the PNIPAAm-COOH was dried in vacuum at 40 °C for 24 h. The monomer conversion (X, %) was calculated as follows:

$$X = (W_2 - N_{COOH} \times M_{CPA}) \times 100/W_1 \quad (1)$$

where W_1 is the weight of the added NIPAAm monomer; W_2, the weight of the produced PNIPAAm-COOH polymer; N_{COOH} is the total molar number of the terminal 4-cyanopentanoic acid in the polymer product, which was determined by back-titration method using excess 0.10 N KOH and then titrated with 0.10 N HCl. The exact concentration of NaOH was calibrated by 0.10 N potassium hydrogen phthalate (KHP). The M_{CPA} is the molecular weight of the CPA, i.e. 126.

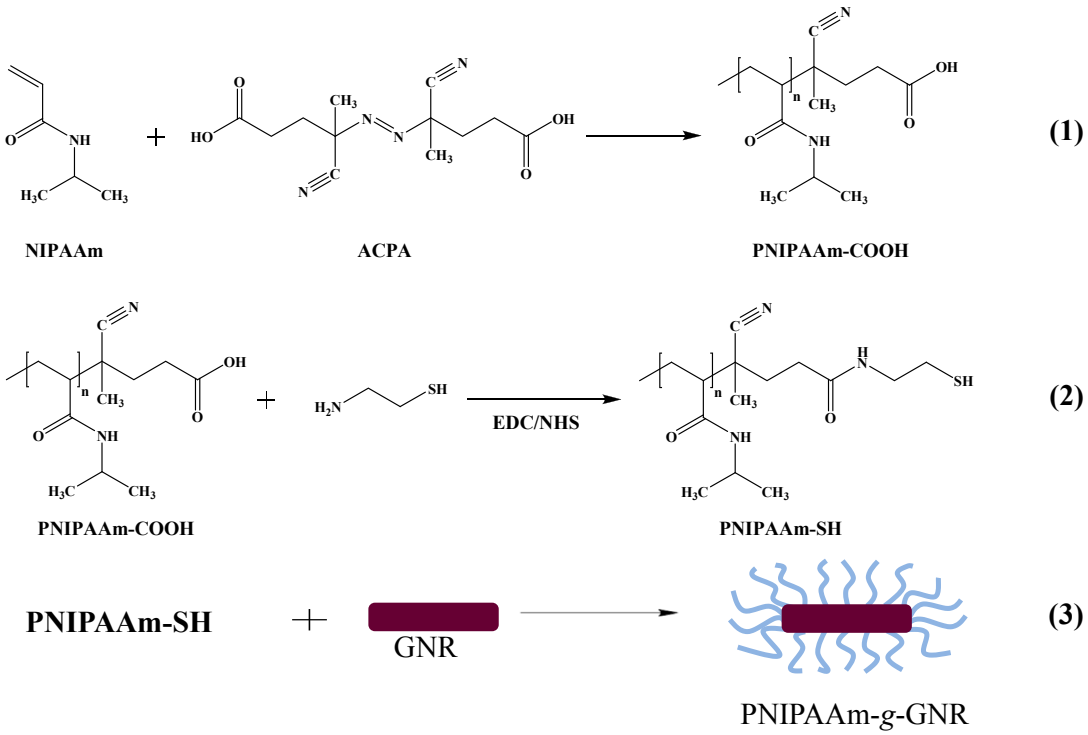

Scheme 1. Preparation of thermo-responsive PNIPAAm-*g*-GNR.

2.3. Synthesis of PNIPAAm-SH

The produced PNIPAAm-COOH (1 g) was dissolved in 50 mL of distilled water and the pH of the solution was adjusted to pH 5. Subsequently, EDC and NHS were added into the PNIPAAm-COOH solution, and stirred for 45 min to activate the terminal carboxylic acid groups of the PNIPAAm-COOH chains. Afterward, the cysteamine was added into the polymer solution, and stirred at room temperature for 4 h to produce the PNIPAAm-SH through the amidation. The reactions are shown in Scheme 1. The EDC, NHS and cysteamine were added in various amounts in order to obtain the maximum yield of the PNIPAAm-SH. To purify the PNIPAAm-SH, the polymer solution was dialyzed first against the 1 mM $HCl_{(aq)}$ solution in the dark, then the mixture solution of 1 mM $HCl_{(aq)}$ and 1% $NaCl_{(aq)}$, and finally the 0.5 mM $HCl_{(aq)}$ solution, each for one day. After dialysis, the PNIPAAm-SH was lyophilized and stored in the refrigerator at 4 °C to maintain its stability against air oxidation.

2.4. Structure analysis

The chemical structure of the produced PNIPAAm-COOH and PNIPAAm-SH was analyzed by Fourier transform infrared (FTIR) spectrometer. After drying, each sample was mixed with KBr powder and ground by an agate mortar. A given amount of the mixture was used for the preparation of KBr pellet. FTIR spectra were then obtained by scanning the KBr pellets for 32 times between 400 and 4000 cm^{-1} with a resolution of 4 cm^{-1}.

The molecular weight of the telechelic PNIPAAm was determined by gel permeation chromatography (GPC). Sample solution was prepared by dissolving polymer in tetrahydrofuran (THF). Afterward, the sample solution was injected into the GPC equipped with an isocratic pump (Waters model 1515), an RI detector (Waters 2414) and two serial styragel HR columns also from Waters. The flow rate was set at 1.0 mL/min, and the temperature was 40 °C. The reported molecular weight was based on polystyrene standard.

The amount of the terminal thiol group was determined by using the Ellman's reagent (DTNB) [43,44] Specifically, sample solution was prepared by dissolving 10 mg of PNIPAAm-SH powder in 6 mL sodium phosphate solution (50 mM, pH = 7). Subsequently, 400 μL of 10% (w/v) $NaBH_4$ solution was added dropwise into the 500 μL sample solution. It was placed in vortex at 37 °C for 1 h. The left $NaBH_4$ was neutralized with 1 mL of 1 M $HCl_{(aq)}$ solution, and the pH value was then adjusted by adding 1 mL of 0.5 M sodium phosphate buffer (pH = 8). Finally, the Ellman's reagent (DTNB) in 100 μL was added to the solution, and the reaction proceeded for 15 min under stirring. The aromatic disulfide in DTNB reacted with the terminal thiol groups in polymer to form a mixed disulfide and 1 mol of 2-nitro-5-thiobenzoate anion (TNB^{2-}) per mole of PNIPAAm-SH. The TNB^{2-} gave an intense yellow color at 412 nm which was quantitatively analyzed by using a UV–Visible spectrophotometer (Helios α, ThermoFisher, USA).

2.5. Determination of lower critical solution temperature (LCST)

The LCST or the cloud point of the telechelic PNIPAAm polymers was determined from the measurement of light transmittance at various temperatures. Sample solution was prepared by dissolving 30 mg polymer in 3 mL distilled water. The light transmittance of the solution at 450 nm was measured at different temperatures using a UV–visible spectrophotometer equipped with a heating cell. The LCST was then determined by the differential peak temperature of the optical transmittance curve.

2.6. Preparation of gold nanorod (GNR)

The GNR was synthesized following the well-known seed-mediated growth method [45,46] with a slight modification. The seed solution was prepared by mixing the $HAuCl_4$ solution (0.25 mL, 0.01 M) with 7.5 mL of 0.10 M CTBA solution. Subsequently, 0.60 mL of 0.010 M $NaBH_4$ solution was added, followed by

a vigorous stirring for 2 min. The resulting seed solution with a brownish yellow color was kept at 28 °C.

For the preparation of growth solution, 0.60 mL of 0.01 M $HAuCl_4$ solution was mixed with 14.25 mL of 0.10 M CTAB solution. To this solution, $AgNO_3$ solution (0.12 mL, 0.01 M) and ascorbic acid solution (0.096 mL, 0.10 M) were added. Ascorbic acid changed the growth solution from brownish yellow to colorless. Finally, the seed solution (0.063 mL) was added to the growth solution, followed by gentle stirring for 10 min. The solution was then kept at 28 °C for 24 h to obtain the GNR. In order to purify the GNR, the mixture solution was dialyzed ($MW_{cut\text{-}off}$ = 6000–8000) against the distilled water for two days to remove the redundant surfactant and unreacted reactants. The produced GNR was stored at 4 °C.

2.7. Preparation of thermo-responsive PNIPAAm-g-GNR composites

The thermos-responsive PNIPAAm-*g*-GNR was prepared by grafting PNIPAAm-SH onto the surface of GNR. In order to enhance the grafting efficiency, the CTAB on the surface of GNR was removed as much as possible by centrifugation at 24140 (×g) twice. Afterwards, the PNIPAAm-SH at various amounts was added into the GNR solution, and followed by gently stirring for 24 h to obtain the PNIPAAm-*g*-GNR composite particles. The unreacted polymers were removed from the PNIPAAm-*g*-GNR solution also by repeated centrifugation at 24140 (×g). The recipes for synthesizing the PNIPAAm-*g*-GNR and their sample codes are listed in Table 1.

2.8. Morphology observation

Sample solution was dripped onto a copper-grid coated with a collodion. It was first dried at room temperature and then vacuum-dried for one day. The morphology of the GNR and PNIPAAm-*g*-GNR particles was then observed by using a transmission electron microscope (TEM, JEOL JEM-2100F-HR).

2.9. Opto-thermal effect of PNIPAAm-g-GNR

The PNIPAAm-*g*-GNR solution (1.5 mL, Abs. = 0.75) was filled into a quartz cell and irradiated for 15 min by a diode laser (808 nm) at a distance of 15 cm. During irradiation, an electronic thermocouple was used to measure the temperature change of the PNIPAAm-*g*-GNR solution every 30 s. Moreover, in order to evaluate its reversibility in opto-thermal property, the PNIPAAm-*g*-GNR solution in a quartz cell was irradiated by a diode laser at a power of 500 mW. After irradiation for 5 min, the diode laser was turned off, and the optical transmission of the PNIPAAm-*g*-GNR solution at 640 nm was immediately recorded by a UV–visible spectrophotometer. After 5 min of measurement, the diode laser was turned on again and continued for another 5 min. The procedure was repeated for 5 times to investigate the reversibility of opto-thermal property of the PNIPAAm-*g*-GNR solution.

Table 1
Recipes and sample codes for the synthesis of PNIPAAm-*g*-GNR.[a]

Sample	GNR		PNIPAAm-SH (μmol)
	Conc. (nM)	Volume (mL)	
PNSGNR1	4.64	3	1.25
PNSGNR2	4.64	3	2.50
PNSGNR3	4.64	3	3.75

[a] For comparison, PNIPAAm-COOH was also used to incubate with the GNR to prepare PNCGNR.

2.10. Cellular compatibility and MTS assay

L929 (ATCC CCL 1) is a fibroblast-like cell line cloned from strain L which is derived from normal subartaneous areolar and adipose tissue of a male C3H/An mouse. The PNIPAAm-*g*-GNR solution (10 μL) and the L929 cell (5×10^3 cell/well) suspended in 100 μL culture medium (HG-DMEM, Sigma–Aldrich, USA) were placed in wells of a 24-well tissue culture polystyrene plate (Corning, Action, MA, USA). Cells were cultured in a humidified incubator balanced with 5% CO_2 at 37 °C. After two days of culture, the cell viability of fibroblasts was determined by MTS assay (Cell Titer 96 Aqueous One Solution, Promega, USA). Each well was dispensed with 100 μL DMEM culture medium and 20 μL MTS using a micropipette and then incubated at 37 °C for 4 h. The absorbance at 490 nm was measured using an enzyme-linked immunosorbent assay (ELISA) with a Multiskan Spectrum microplate spectrophotometer (Thermo science, UK), and it was then converted directly to the cell number using a standard curve. Data were collected and averaged from five measurements.

3. Results and discussion

3.1. Structure analysis of telechelic PNIPAAm-COOH polymer

In order to confirm the structure of the produced PNIPAAm-COOH initiated by ACPA, its FTIR spectrum was compared to that of pure PNIPAAm synthesized by using azobisisobutyronitrile (AIBN) as initiator. Fig. 1 shows that both PNIPAAm polymers initiated by AIBN and ACPA have the same characteristic absorption peaks such as C=O stretching vibration (amide I) at 1648 cm^{-1}, and N–H bending vibration (amide II) at 1542 cm^{-1}, in addition to the splitting absorption peaks of isopropyl group at 1387 cm^{-1} and 1367 cm^{-1}, and the methyl absorption peaks at 2972 cm^{-1} and 2876 cm^{-1}. Yet, a particular shoulder at 1715 cm^{-1} is found in Fig. 1(c), owing to the added ACPA initiator (cf. Fig. 1(b)). During the reaction, the ACPA initiator was thermally dissociated into two radicals that could initiate the polymerization, resulting in the polymer chains end-capped with the carboxylic acid group as shown in Scheme 1. Therefore, the FTIR analysis demonstrates the structure of PNIPAAm-COOH. For the present reaction system, the conversion and the molecular weight are found to be 87% and 6180 g/mol, respectively. The amount of the terminal acid groups determined by back-titration is 0.248 mmol/g.

3.2. Synthesis and structure analysis of PNIPAAm-SH polymer

In order to graft the PNIPAAm onto the gold nanorod, the synthesized PNIPAAm-COOH was further converted to the PNIPAAm-SH through amidation with cysteamine using NHS/EDC as activated compounds. It is known that the amidation via the NHS/EDC depends on the pH value of the solution. From several preliminary experiments, we found out that pH5 would give the maximum yield of the thiol-end- group for the present system. At a lower pH value of 4, the reactivity of EDC would be lower; while at a higher pH value of 6, most COOH groups in the PNIPAAm-COOH would be ionized to form the COO^- so as to reduce their reactivity. Both situations thus decreased the yield of thiol-end-group. In addition, the optimum molar ratios of the EDC and NHS relative to the terminal COOH were found to be 4.0 and 2.4, respectively. After activation, the cysteamine was then added at the twice molar amount of COOH. The reaction was continued for 4 h under a pH5 environment to obtain PNIPAAm-SH. The structure of the reaction product was then identified by FTIR spectrum. Fig. 2(a) and (b) show the FTIR spectra of PNIPAAm-COOH and PNIPAAm-SH, respectively. The original C=O absorption peak at 1715 cm^{-1} in

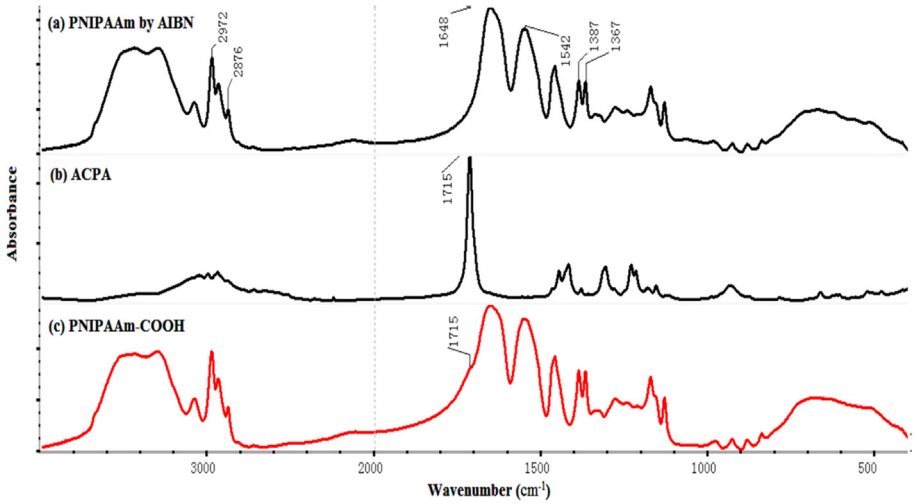

Fig. 1. FTIR spectra of (a) PNIPAAm synthesized by using AIBN as initiator (b) ACPA (c) PNIPAAm-COOH synthesized by using ACPA as initiator. AIBN: azobisisobutyronitrile, ACPA: 4,4′-azobis(4-cyanopentanoic acid).

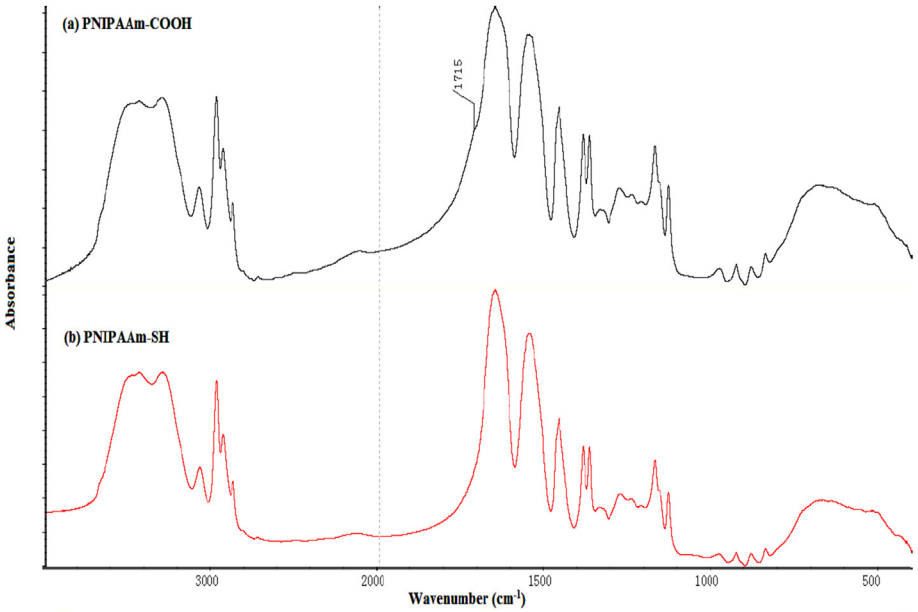

Fig. 2. FTIR spectra of (a) PNIPAAm-COOH and (b) PNIPAAm-SH (reaction condition: [COOH]/[EDC]/[NHS]/[NH_2] = 1/4/2.4/2 and reaction for 4 h at pH5).

the PNIPAAm-COOH spectrum disappeared in the spectrum of the PNIPAAm-SH, indicating that the terminal acid group was reacted with the cysteamine via the amidation reaction. However, due to the little amount of the thiol-end-group and its weak absorption, the absorption peaks of the thiol group could not be clearly observed in the spectrum of PNIPAAm-SH. The thiol group could be identified by the TEM/EDX which will be discussed in the later section. Furthermore, by reacting PNIPAAm-SH with the Ellman's reagent (DTNB) [43,44] which produced TNB^{2-} with an intense yellow color at 412 nm, the amount of the terminal thiol groups in the polymer chains was thus determined. The amount of terminal SH group in the produced PNIPAAm-SH was about 28.32 μmol/g-polymer. In other words, the substitution degree was 11.4%. Though the value seems to be low, it is still higher than the reported values [44,47]. Verheul et al. [44] found the degrees of substitution were only 5–7% for the thiolation of partially carboxylated trimethyl chitosan.

3.3. The LCST of PNIPAAm-COOH and PNIPAAm-SH

The LCST of the synthesized PNIPAAm-COOH is about 35.4 °C determined by optical transmittance at 450 nm as shown in Fig. 3. This value is slightly higher than the generally reported LCST for the neat PNIPAAm, i.e. 32 °C. This is because the attached hydrophilic end group of COOH. After amidation reaction to convert the acid group to the thiol group, it can be seen that the LCST of the PNIPAAm-SH is 35.1 °C, nearly the same as that of the PNIPAAm-COOH. This indicates that the thiol end group is almost as hydrophilic as the carboxylic acid group. We also changed the amount of thiol end group by changing the molar ratio of [NH_2]/[COOH] and

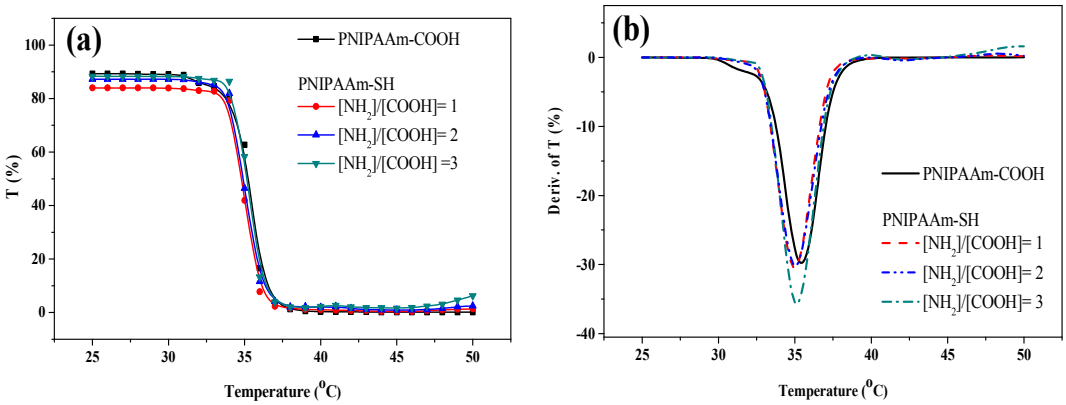

Fig. 3. (a) Optical transmittance curves at 450 nm and (b) their differential peaks for the PNIPAAm-COOH and its derivatives of PNIPAAm-SHs obtained at different molar ratios of $[NH_2]/[COOH]$ in the feed.

the effect on the LCST is minimal indicating that the COOH and SH groups have nearly the same hydrophilicity.

3.4. The morphology of GNR

The GNR was synthesized by seed-mediated growth method [45,46]. Fig. 4(a) and (b) show the morphology the GNR. A well-defined rod structure is observed with the length and wide being 37.23 (±0.91) nm and 11.15 (±0.29) nm, respectively. The aspect ratio (AR) thus is 3.34 ± 0.12. Because of its surface plasmon resonance (SPR), Fig. 4(c) shows that there are two absorption peaks with their λ_{max} at 525 and 801 nm in the spectrum, owing to the transverse and longitudinal SPR, respectively. The longitudinal $\lambda_{max,L}$ in the near-IR region is particularly important in this study and its intensity is much higher than that of the transverse $\lambda_{max,T}$. It is known that the $\lambda_{max,L}$ would red-shift to a higher wavenumber as the AR is raised. In aqueous solution, the longitudinal SPR $\lambda_{max,L}$ is linearly proportional to the aspect ratio (AR) by the following relationship:[48]

$$\lambda_{max,L} = 95 \times AR + 420(nm)$$

According to the above equation, the calculated AR from the spectrum is 3.98, about 19% higher than the value from the TEM.

3.5. Morphology and optical absorbance of PNIPAAm-g-GNR composites

After the synthesis of GNR, the PNIPAAm-SH was tried to graft onto the surface of the GNR to protect the GNR and also to provide the thermo-sensitive property. First, the prepared GNR solution was centrifuged twice to remove the CTAB surfactant on the GNR surface. The PNIPAAm-SH was then added to the GNR solution. The grafting reaction underwent at room temperature for 24 h. Finally, it was centrifuged again for two times to obtain the PNIPAAm-*g*-GNR. The zeta potential for the original GNR is 50.6 mV and decreases to 13.1 mV for the PNSGNR1 (see Table 1), suggesting the successful replacement of CTAB by PNIPAAm. And increasing the added amount of PNIPAAm-SH would further decrease the zeta potential of the produced PNIPAAm-*g*-GNR, where the zeta potential becomes 9.23 mV for the PNSGNR3. The decrease in the zeta potential thus implies that the PNIPAAm is grafted onto the surface of GNR.

In order to prove that the PNIPAAm chains were grafted onto GNR, FTIR spectra of various PNIPAAm-*g*-GNR samples were taken. Fig. 5(a) shows a typical FTIR spectrum of the PNIPAAm-*g*-GNR samples; it clearly reveals all the characteristic absorption peaks of the PNIPAAm chains. All the characteristic bands of PNIPAAm, PNIPAAm-COOH, PNIPAAm-SH and PNIPAAm-g-GNR with identification of functional groups are summarized in Table 2. Furthermore, a TEM picture of the PNIPAAm-*g*-GNR is shown in Fig. 5(b). Around the GNR, gray coating is observed. By using a technique of line-scan in TEM/EDX for elemental analysis across the GNR, it can be seen in Fig. 5(c) that the signal of sulfur is in accordance with the trace of gold, indicating that the sulfur is bonded and only can be observed on the surface of GNR. On the other hand, the oxygen element in the grafted PNIPAAm chains can be seen all around the GNR with the same intensity. Therefore, the FTIR and TEM pictures prove the grafting of the PNIPAAm chains onto the GNR. After grafting, it is also important to understand the stability of the PNIPAAm-*g*-GNR which is indicated by the variation of maximum absorption wavelength and its absorbance in the UV–Visible spectra with time. Fig. 5(d) shows that there is nearly no change in the spectra of the PNIPAAm-*g*-GNR after 5 days of storage; the

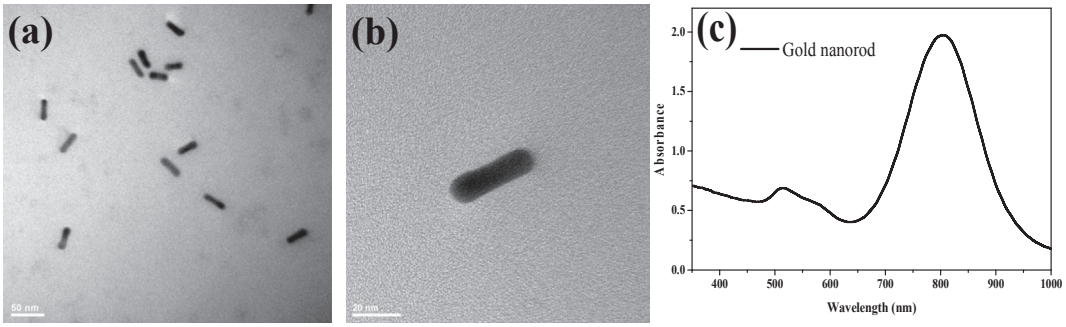

Fig. 4. TEM pictures of GNR at magnifications of (a) ×160 k, (b) ×600 k; and (c) UV–visible spectrum of GNR.

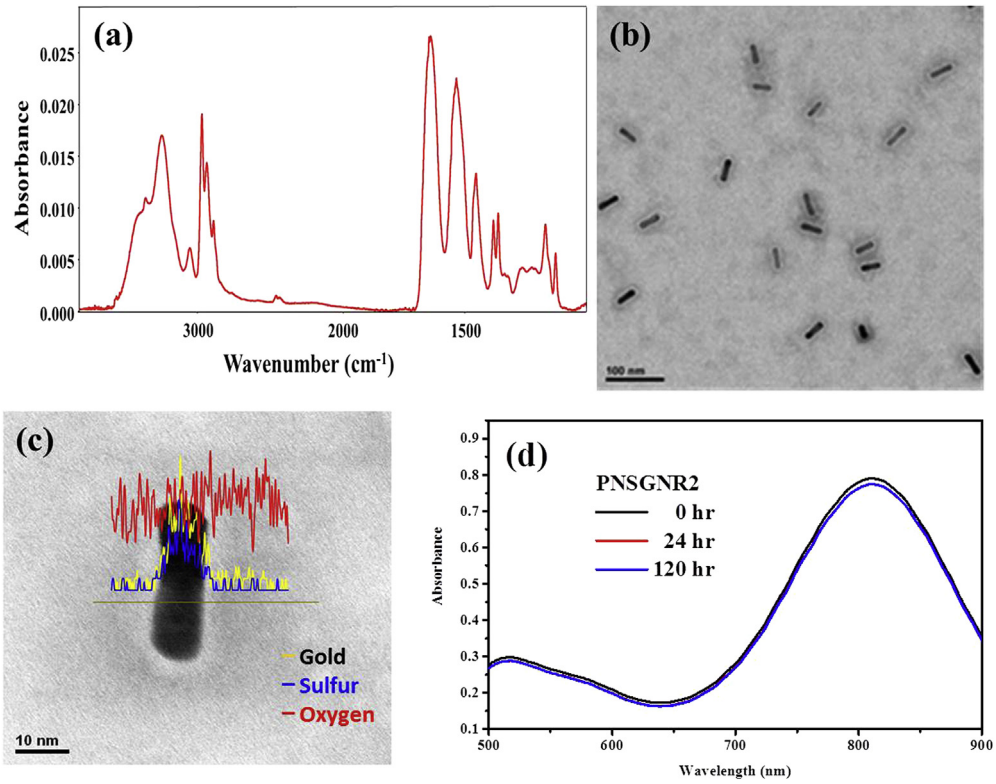

Fig. 5. (a) A typical FTIR spectrum of the PNIPAAm-*g*-GNR (b) TEM micrograph of the PNIPAAm-*g*-GNR at room temperature (the bar is 100 nm), (c) element distribution across the PNIPAAm-*g*-GNR using line-scan in TEM/EDX (the bar is 10 nm), and (d) the change of optical absorption of the PNIPAAm-*g*-GNR solution with time. The PNSGNR2 was taken for example.

Table 2
Characteristic absorption peaks of PNIPAAm, PNIPAAm-COOH, PNIPAAm-SH and PNIPAAm-*g*-GNR in their FTIR spectra.

Functional group	PNIPAAm[a]		PNIPAAm-COOH		PNIPAAm-SH		PNIPAAm-g-GNR[b]	
	$\bar{\upsilon}$ (cm^{-1})	Abs.	$\bar{\upsilon}$ (cm^{-1})	Abs.	$\bar{\upsilon}$ (cm^{-1})	Abs.	$\bar{\upsilon}$ (cm^{-1})	Abs.
$-CH_3$	2972	0.420	2975	0.420	2974	0.420	2971	0.0254
	2876	0.199	2877	0.194	2876	0.159	2875	0.0147
$-CH_2$	2933	0.315	2936	0.303	2935	0.277	2931	0.0204
−COOH	–	–	1715	0.357	–	–	–	–
C=O (amide I)	1648	0.654	1653	0.614	1652	0.707	1645	0.0324
N–H (amide II)	1542	0.557	1556	0.556	1551	0.596	1539	0.0293
$>C(CH_3)_2$	1387	0.324	1388	0.334	1388	0.302	1386	0.0170
	1367	0.324	1368	0.334	1368	0.302	1367	0.0178

[a] For PNIPAAm, PNIPAAm-COOH and PNIPAAm-SH, samples were separately mixed with KBr powder and pressed into disks. Transmission mode was used to obtain their FTIR spectra. For comparison, all the absorbance values (Abs.) are normalized based on the methyl absorption peak.
[b] For PNIPAAm-g-GNR, attenuated total reflection (ATR) mode was used to obtain its FTIR spectrum.

maximum absorption wavelength λ_{max} remained the same and the absorbance at the peak only decreased by 1.9% after 5 days, indicating that the GNRs were protected by PNIPAAm chains from aggregation and all three PNSGNR samples have similar stability. A red shift from 801 nm to 810 nm was observed for the longitudinal $\lambda_{max,L}$ of all three PNIPAAm-*g*-GNR (PNSGNR1, PNSGNR2 and PNSGNR3) in comparison with that of the original CTAB-stabilized GNR. This is consistent with the AuNPs bonded with PEG−SH shells reported by Shultz et al. [18] and was attributed to a change of the dielectric environment at the gold surface.

3.6. Thermo-responsive properties of the PNIPAAm-g-GNR

Following the confirmation of the PNIPAAm chains being successfully grafted onto the GNR, the thermos-responsive properties of the PNIPAAm-*g*-GNR was investigated. The phase transition temperature as denoted by LCST can be determined by the transition of optical transmittance as a function of temperature. Fig. 6(a) shows identical optical transmittance curves for the PNIPAAm-SH and PNIPAAm-*g*-GNR, indicating that the GNR has minimal effects on the LCST of the PNIPAAm. Fig. 6(b) reveals that the LCST as indicated by the differential peak temperature is located at 34.9 °C. Above this temperature, the PNIPAAm-*g*-GNR solution becomes translucent due to the aggregation of the grafted PNIPAAm chains. The morphologies of the PNIPAAm-*g*-GNR at temperatures below and above its LCST were also examined by TEM. At room temperature (lower than the LCST), the gold nanorods were well-dispersed and separated from each other as shown in Fig. 6(c). When the temperatures was above the LCST (at 40 °C) and dried on the carbon-supported grid, the PNIPAAm chains agglomerated into

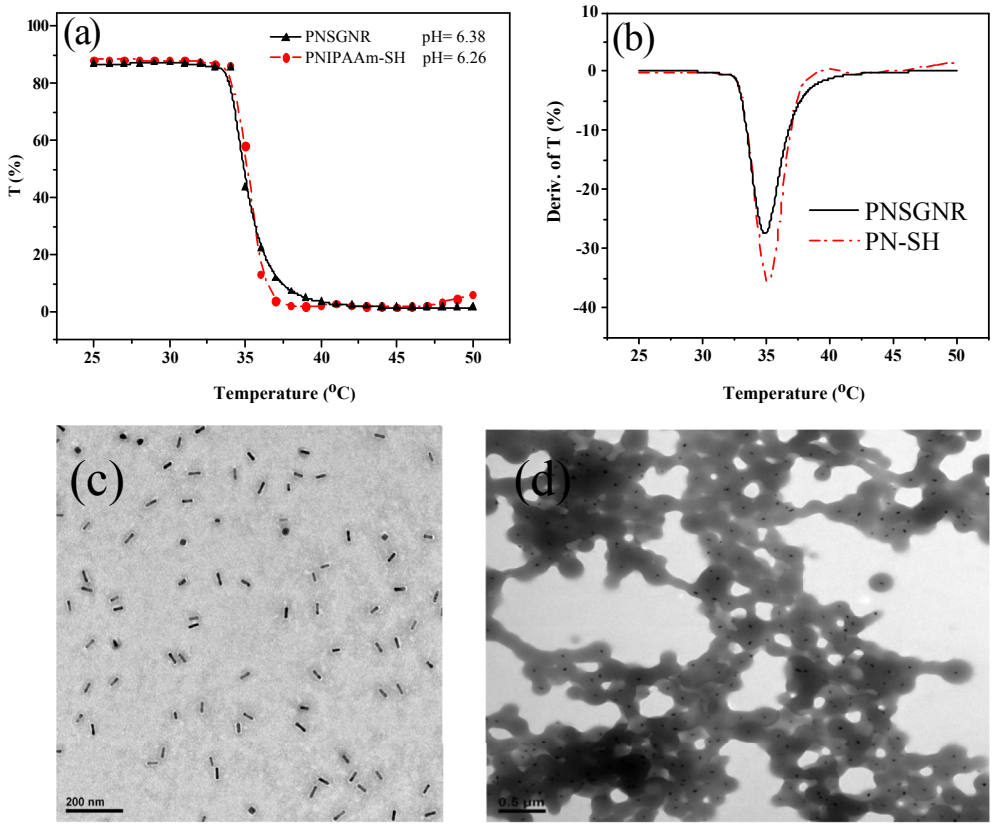

Fig. 6. (a) Optical transmittance curves and (b) their differential peaks for the PNIPAAm-*g*-GNR (PNSGNR2) and PNIPAAm-SH; TEM micrographs of the PNIPAAm-*g*-GNR (PNSGNR2) (c) at room temperature (the bar is 200 nm), and (d) at 40 °C (the bar is 500 nm).

network as they become hydrophobic as shown in Fig. 6(d). In addition, each tiny GNR can be seen as located at the center of individual spherical PNIPAAm cloud. For comparison purpose, we also incubated the PNIPAAm-COOH with the GNR following the same procedure as described in the experimental section. The TEM picture showed that the PNIPAAm formed its own agglomeration, independent of the location of the GNRs indicating that the PNIPAAm-COOH did not bind to the GNR and thus could not stabilize the GNR (see Supplementary Fig. S1).

The reversibility is evaluated by the SPR absorbance and phase transition behavior of the PNIPAAm-*g*-GNR during several heating-and-cooling cycles between 25 and 40 °C. Fig. 7(a) shows that the UV–visible spectra of the PNIPAAm-*g*-GNR were invariant through 5 thermal cycles, indicating that the SPR effects of the GNR are not affected by the thermo-induced aggregation and re-dispersion. Moreover, the light transmittance at 640 nm was measured for the PNIPAAm-*g*-GNR solution repeatedly between 25 °C and 40 °C during thermal cycles as shown in Fig. 7(b). Reversibility of the PNIPAAm-*g*-GNR through the thermo-cycle was also observed. It also can be deduced from the above results that strong chemical bonding exists between the PNIPAAm chains and GNR which is not affected by the repeated heating-and-cooling cycles between 25 and 40 °C.

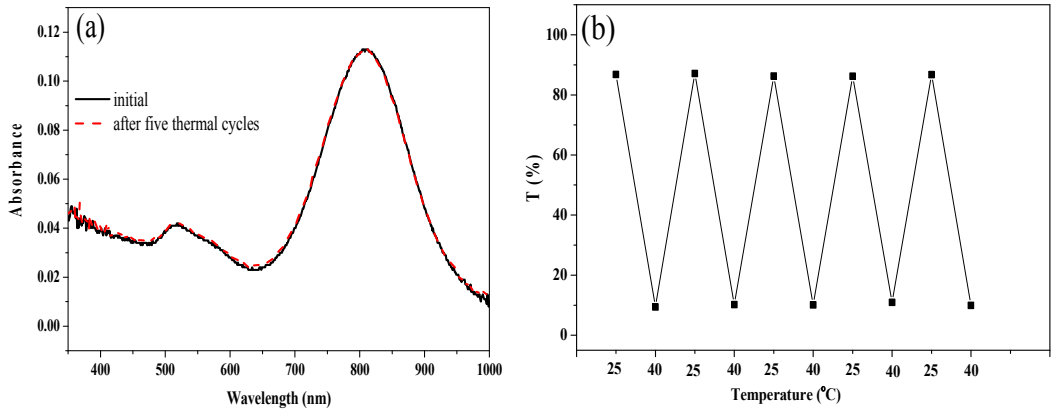

Fig. 7. (a) UV–visible spectra of the PNIPAAm-*g*-GNR (PNSGNR2) before and after five heating-and-cooling cycles from 25 to 40 °C; (b) optical transmittance of the PNIPAAm-*g*-GNR solution measured repeatedly at 25 °C and 40 °C during thermal cycles.

3.7. The opto-thermal effect of PNIPAAm-g-GNR composites

In this study, the diode laser at 808 nm was used as the light source to irradiate the PNIPAAm-*g*-GNR solution so as to induce its characteristic opto-thermal effect. The distilled water was used as the control. Fig. 8(a) shows that an increase of 11.7 °C is observed when the diode laser with 300 mW is used to illuminate the PNSGNR2 solution for 15 min, while only a half increment is found for the distilled water. Moreover, increasing the diode-laser power increases the opto-thermal effect. With an irradiation of 500 mW, the temperature increases from original 26.1 °C–44.9 °C, an increment of 18.8 °C for the PNSGNR2 solution as shown in Fig. 8(b). It is also noticed that after 5 min of irradiation, the temperature already increases to 36.5 °C, higher than the LCST of the PNIPAAm-*g*-GNR. In other words, we can irradiate the PNIPAAm-*g*-GNR solution to induce the opto-thermal effect that could raise the temperature to above its LCST and thus causes the phase transition of the polymer.

Furthermore, reversibility in opto-thermal property was also examined while a diode laser at a power of 500 mW was used to irradiate the PNIPAAm-*g*-GNR solution for the first 5 min. It was then turned off, and the optical transmission of the solution at 640 nm was immediately recorded. After 5 min of measurement, the diode laser was turned on again and repeated the procedure at least 5 times. Fig. 9 shows that the opto-thermal effect is completely reversible. Once the diode laser is turned off, the PNIPAAm-*g*-GNR solution gradually turns into transparent, and therefore the optical transmittance starts to increase and finally reaches 100% in about 1.75 min. This is consequently because the grafted PNIPAAm chains change from the collapsed and aggregation state to the hydrated and dissolved state as the temperature gradually decreases to below its LCST. When the diode laser is turn on again and continued for another 5 min, the solution temperature is continuously increased and finally raised to a temperature above its LCST as shown in the previous Fig. 8(b). The solution thus becomes opaque with a very low light transmittance. The complete reversibility in opto-thermal behavior indicates that the repeated morphology changes in the grafted PNIPAAm chains would not affect the SPR effects of the GNR.

3.8. Cellular compatibility of CTAB-GNR and PNIPAAm-g-GNR

L929 (ATCC CCL 1) is a fibroblast-like cell line cloned from strain L which was derived from normal subartaneous areolar and adipose tissue of a male C3H/An mouse. The PNIPAAm-*g*-GNR solution (10 μL) and the L929 cell (5×10^3 cell/well) suspended in 100 μL culture medium (HG-DMEM, Sigma–Aldrich, USA) were placed in wells of a 24-well tissue culture polystyrene plate (Corning, Action, MA, USA). Cells were cultured in a humidified incubator balanced with 5% CO_2 at 37 °C. After two days of culture, the cell viability of fibroblasts was determined by MTS assay (Cell Titer 96 Aqueous One Solution, Promega, USA). Each well was dispensed with 100 μL DMEM culture medium and 20 μL MTS using a micropipette and then incubated at 37 °C for 4 h. The absorbance at 490 nm was measured using an enzyme-linked immunosorbent assay (ELISA) with a Multiskan Spectrum microplate spectrophotometer (Thermo science, UK), and it was then converted directly to the cell number using a standard curve. Data were collected and averaged from five measurements.

To study the cytotoxicity of GNR and PNIPAAm-grafted GNR, the L-929 cells were cultured in the culture medium at the presence of GNR and PNIPAAm-*g*-GNR particles for two days respectively. For comparison, the cell culture in the nutrition medium only was used as the control. The cell viability of L-929 cells was then measured by the method of MTT assay. It can be seen in Fig. 10 that the cell viability of L-929 cultured with the GNR almost approaches to zero. This is because the GNR is stabilized by CTAB which is cytotoxic. Yet, as the GNR is centrifuged to remove the CTAB surfactant and replaced by PNIPAAm, the L-929 cultured in the prepared

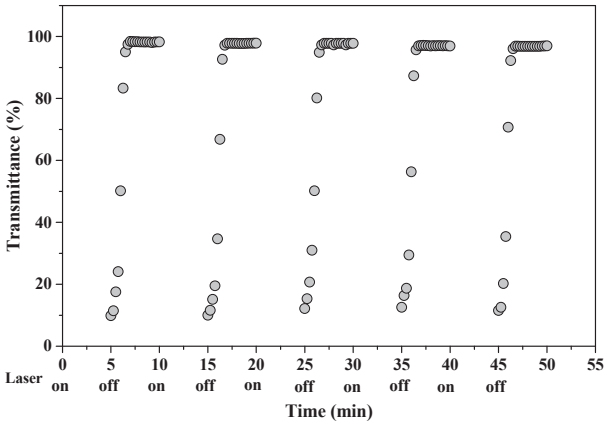

Fig. 9. Optical transmittance of the PNIPAAm-*g*-GNR (PNSGNR2) measured immediately after turn-off of the diode laser during the repeated turn-on and turn-off cycles.

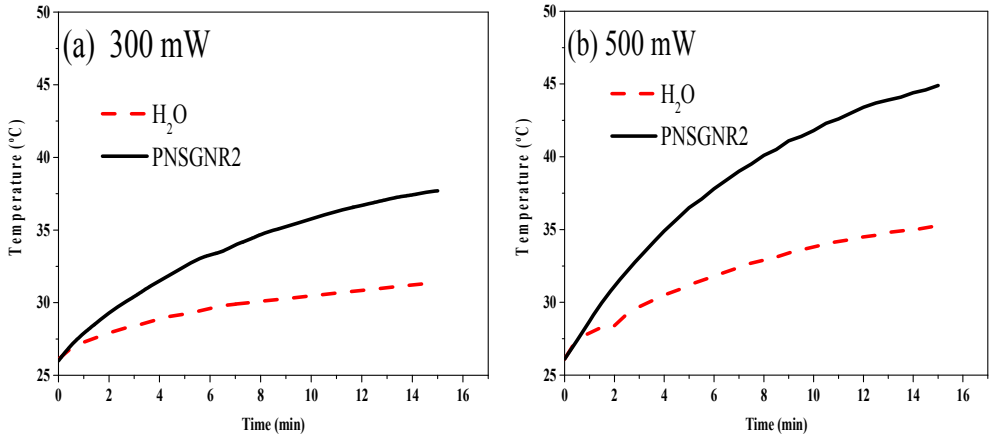

Fig. 8. The temperature increment of the PNIPAAm-*g*-GNR solution and the distilled water during the continuous irradiation of a diode laser (808 nm) at (a) 300 mW, and (b) 500 mW.

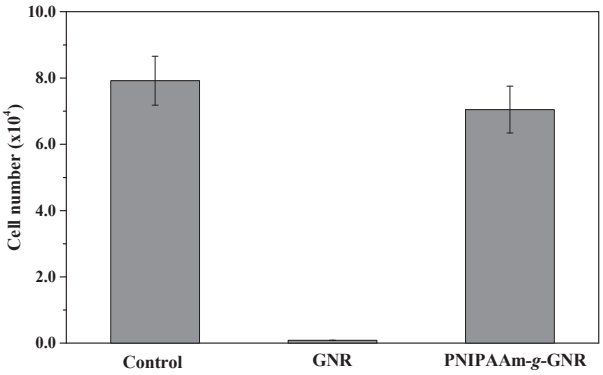

Fig. 10. Cell viability of L-929 cells in the culture medium at the presence of GNR and PNIPAAm-*g*-GNR (PNSGNR2) measured by the method of MTS assay. The control group is the cell culture in the medium only.

PNIPAAm-*g*-GNR solution has almost the same cell viability as cultured in the control. This is beneficial for the application of the PNIPAAm-*g*-GNR in the biomedical field.

4. Conclusion

In this study, the thermo-responsive PNIPAAm-protected GNRs were successfully synthesized by chemically grafting the PNIPAAm-SH to the GNRs through the thiol bonding on the gold surface. These GNRs were synthesized via the well-known seed-mediated growth method and had an average aspect ratio of 3.34 accompanied with a longitudinal SPR absorbance ($\lambda_{max,L}$) at 801 nm in the NIR region. After grafting with the PNIPAAm, a red-shift to 810 nm was observed. The PNIPAAm chains could prevent the GNRs from aggregation, allowing the PNIPAAm-protected GNRs to be stable in the aqueous medium with the invariant UV–visible absorbance spectrum. However, the agglomeration of PNIPAAm-*g*-GNR was found when the temperature raised above the LCST, i.e., 34.9 °C. The morphological transition was reversible after several heating-and cooling cycles. Because of its opto-thermal properties, the increment in temperature could be achieved by irradiation of near-IR light on the PNIPAAm-*g*-GNR. Last but not least, the cytotoxicity of PNIPAAm-*g*-GNR was greatly reduced in comparison with the CTAB-stabilized GNR. Therefore, the thermo-responsive PNIPAAm-*g*-GNR could be used as the controlled drug-release carriers controlled by remote near-IR.

Acknowledgments

Grant-in-aid from Taiwan under the contract number of MOST 104-2221-E-032 -052 -MY3 is greatly appreciated. We also like to thank Ms. Ching-Yen Lin in National Taiwan University for her help in taking the TEM pictures.

Appendix A. Supplementary data

Supplementary data related to this article can be found at http://dx.doi.org/10.1016/j.polymer.2015.12.047.

References

[1] G. Han, P. Ghosh, M. De, V.M. Rotello, Nanobiotechnol 3 (2007) 40–45.
[2] S.E. Skrabalak, J. Chen, L. Au, X. Lu, X. Li, Y. Xia, Adv. Mater. 19 (2007) 3177–3184.
[3] S. Lal, S.E. Clare, N.J. Halas, Acc. Chem. Res. 41 (2008) 1842–1851.
[4] L. Tong, Q.S. Wei, A. Wei, J.X. Cheng, Photochem Photobiol. 85 (2009) 21–32.
[5] T. Nann, Nano Biomed. Eng. 3 (2011) 137–143.
[6] D.P. O'Neal, L.R. Hirsch, N.J. Halas, J.D. Payne, J.L. West, Cancer Lett. 209 (2004) 171–176.
[7] K.Y. van Berkel, C.J. Hawker, J. Polym. Sci. Part A Polym. Chem. 48 (2010) 1594–1606.
[8] L.M. Liz-MarzKn, M. Giersig, P. Mulvaney, Langmuir 12 (1996) 4329–4335.
[9] I. Pastoriza-Santos, J. Pmrez-Juste, L.M. Liz-MarzKn, Chem. Mater. 18 (2006) 2465–2467.
[10] C. Lofton, W. Sigmund, Adv. Funct. Mater. 15 (2005) 1197–1208.
[11] N. Malikova, I. Pastoriza-Santos, M. Schierhorn, N.A. Kotov, L.M. Liz-MarzKn, Langmuir 18 (2002) 3694–3697.
[12] F. Kim, S. Connor, H. Song, T. Kuykendall, P. Yang, Angew. Chem. 116 (2004) 3759–3763.
[13] C.L. Nehl, H. Liao, J.H. Hafner, Nano Lett. 6 (2006) 683–688.
[14] N.R. Jana, L. Gearheart, C.J. Murphy, J. Phys. Chem. B 105 (2001) 4065–4067.
[15] H.W. Liao, J.H. Hafner, Chem. Mater. 17 (2005) 4636–4641.
[16] C. Kojima, H. Kawabata, A. Harada, H. Horinaka, K. Kono, Chem. Lett. 42 (2013) 612–614.
[17] L. Ramin, A. Jabbarzadeh, Langmuir 28 (2012) 4102–4112.
[18] F. Schulz, T. Vossmeyer, N.G. Bastús, H. Weller, Langmuir 29 (2013) 9897–9908.
[19] H. Chen, Y. Wang, Y. Wang, S. Dong, E. Wang, Polymer 47 (2006) 763–766.
[20] K. Ohno, K. Koh, Y. Tsujii, T. Fukuda, Macromolecules 35 (2002) 8989–8993.
[21] C. Mangeney, F. Ferrage, I. Aujard, V. Marchi-Artzner, L. Jullien, O. Ouari, El D. Rékaï, A. Laschewsky, I. Vikholm, J.W. Sadowski, J. Am. Chem. Soc. 124 (2002) 5811–5821.
[22] M.K. Corbierre, N.S. Cameron, R.B. Lennox, Langmuir 20 (2004) 2867–2873.
[23] N. Bogliotti, B. Oberleitner, A. Di-Cicco, F. Schmidt, J.C. Florent, V. Semetey, J. Colloid Interface Sci. 357 (2011) 75–81.
[24] T. Teranishi, I. Kiyokawa, M. Miyake, Adv. Mater. 10 (1998) 596–599.
[25] J. Shan, M. Nuopponen, H. Jiang, E. Kauppinen, H. Tenhu, Macromolecules 36 (2003) 4526–4533.
[26] F.M. Winnik, Polymer 31 (1990) 2125–2134.
[27] C.K. Chee, S. Rimmer, I. Soutar, L. Swanson, Polymer 42 (2001) 5079–5087.
[28] S. Zhou, B. Chu, J. Phys. Chem. B 102 (1998) 1364–1371.
[29] M. Karg, T. Hellweg, Curr. Opin. Colloid Interface Sci. 14 (2009) 438–450.
[30] R. Contreras-Cáceres, J. Pacifico, I. Pastoriza-Santos, J. Perez-Juste, A. Fernandez-Barbero, L.M. Liz-Marzan, Adv. Funct. Mater. 19 (2009) 3070–3076.
[31] T. Chen, D.P. Chang, J.M. Zhang, R. Jordan, S. Zauscher, Adv. Funct. Mater. 22 (2012) 429–434.
[32] W.Y. Li, X. Cai, C.H. Kim, G.R. Sun, Y. Zhang, R. Deng, M.X. Yang, J.Y. Chen, S. Achilefu, L.V. Wang, Y.N. Xia, Nanoscale 3 (2011) 1724–1730.
[33] X.Q. Zhao, T.X. Wang, W. Liu, C.D. Wang, D. Wang, T. Shang, L.H. Shen, L. Ren, J. Mater. Chem. 21 (2011) 7240–7247.
[34] J.H. Kim, T.R. Lee, J. Biomed. Pharm. Eng. 2 (2008) 29–35.
[35] J. Raula, J. Shan, M. Nuopponen, A. Niskanen, H. Jiang, E. Kauppinen, H. Tenhu, Langmuir 19 (2003) 3499–3504.
[36] M. Karg, Y. Lu, E. Carbo-Argibay, I. Pastoriza-Santos, J. Perez-Juste, L.M. Liz-Marzan, T. Hellweg, Langmuir 25 (2009) 3163–3167.
[37] A. Khan, M. Alhoshan, J. Polym, Sci. Part A Polym. Chem. 51 (2013) 39–46.
[38] T. Shang, C.D. Wang, L. Ren, X.H. Tian, D.H. Li, X.B. Ke, M. Chen, A.Q. Yang, Nanoscale Res. Lett. 8 (2013) 4.
[39] T. Kawano, Y. Niidome, T. Mori, Y. Katayama, T. Niidome, Bioconjug. Chem. 20 (2009) 209–212.
[40] J. Rodríguez-Fernndez, M. Fedoruk, C. Hrelescu, A.A. Lutich, J. Feldmann, Nanotechnology 22 (2011) 245708.
[41] Q. Wei, J. Ji, J. Shen, Macromol. Rapid Commun. 29 (2008) 645–650.
[42] M. Nguyen, X. Sun, E. Lacaze, P.M. Winkler, A. Hohenau, J.R. Krenn, C. Bourdillon, A. Lamouri, J. Grand, G. Levi, L. Boubekeur-Lecaque, C. Mangeney, N. Félidj, ACS Photonics 2 (2015) 1199–1208.
[43] G.L. Ellman, Arch. Biochem. Biophys. 82 (1959) 70–77.
[44] R.J. Verheul, S. Van Der Wal, W.E. Hennink, Biomacromolecules 11 (2010) 1965–1971.
[45] B. Nikoobakht, M.A. El-sayed, Chem. Mater. 15 (2003) 1957–1962.
[46] N.R. Jana, L. Gearheart, C.J. Murphy, Adv. Mater. 13 (2001) 1389–1393.
[47] C.E. Kast, A. Bernkop-Schnürch, Biomaterials 22 (2001) 2345–2352.
[48] X. Huang, S. Neretina, M.A. El-Sayed, Adv. Mater. 21 (2009) 1–31.